Sustainability, transfer and containment properties of concrete subject to delayed ettringite formation (DEF)

Arthur Pichelin, Myriam Carcasses, Franck Cassagnabère, Stéphane Multon, G. Nahas

Sustainability, transfer and containment properties of concrete subject to Delayed Ettringite Formation (DEF).

A. Pichelin[(a,b)], M. Carcassès[(a)], F. Cassagnabère[(a)], S. Multon[(a)], G. Nahas[(b)]

(a) Laboratoire Matériaux et Durabilité des Constructions (LMDC), Toulouse, France.
(b) Institut de Radioprotection et de Sûreté Nucléaire (IRSN), Fontenay-aux-Roses, France.

Abstract

This work used numerous experimental techniques to evaluate the physicochemical and mechanical modifications of concrete damaged by swelling due to internal sulfate attack. The first objective was to determine property sensitive to DEF (delayed ettringite formation) and able to detect it before apparent cracking. The second objective was to quantify the evolution of the properties that impact the containment property and the sustainability of concrete after expansion and damage. It was found that gas permeability, electrical resistivity and static moduli results were the most promising techniques to detect DEF during the latency period. The loss of containment appears for damage lower than 20%.

Keywords: Delayed Ettringite Formation (DEF); Sustainability indicators; Internal Sulfate Attack (ISA); Swelling; Nuclear structure; containment property.

1. Introduction

Internal Sulfate Attack (ISA) can be due to the formation of delayed ettringite (DEF) in cementitious material, after concrete hardening and without external sulfate supply. Many engineering structures are susceptible to develop these pathologies. This reaction requires the presence of three main factors: high sulfate and aluminate contents, water, and a rise in temperature at young age and/or later. The reaction mechanisms of DEF are complex but Brunetaud has proposed a global mechanism, described in four phases, grouping many theories [1]. Several parameters have an influence on the development of DEF, and can be divided into two groups: those related to the formulation of concrete and those related to the environment. Concerning the formulation parameters, the expansion generated is strongly dependent on the nature of the binder, in particular on the sulfate, aluminate and alkali contents [2, 3]. The amount of added water is also influential. It modifies the porosity and therefore the ionic transfer [2, 4]. In addition, the nature and size of aggregates are important; it has been shown that the use of small siliceous aggregates significantly increases the kinetics and the swelling potential of DEF [5, 6]. As far as the environmental conditions are concerned, DEF requires a minimum of 90% relative humidity and a rise in temperature to above 65°C once in its history [7]. Expansion increases with the water content of concrete [8]. In terms of temperature, results from the literature show a combined influence of the maximal temperature and the duration when the temperature is higher than about 65°C [9]. The evaluation of DEF damage in nuclear power plants represents an important economic and societal challenge. The main consequences of DEF are expansion and cracks. They affect the physicochemical and mechanical properties of the concrete. Cracks lead to an increase of transfer properties and a decrease of mechanical properties and may lead to a loss of containment, which is harmful for nuclear power plants. Massive elements can be particularly sensitive to DEF due to the risk of temperature increase at young age caused by the heat production during cement hydration [10]. It therefore becomes necessary to propose a measurement method to assess the state of degradation of the concrete generated by DEF in such elements. Few data can be found in the literature on the evolution of the physicochemical and mechanical properties of concrete according to the degree of advancement of DEF. The present study had two objectives: first, to find a very sensitive test allowing DEF to be detected before cracking can be observed visually and, second, to evaluate the evolution of the properties that impact the containment and also the sustainability of concrete affected by usual concrete pathologies such as carbonation, corrosion, etc. A test protocol to accelerate DEF development was carried out and provided a good representation of the reality on site [11]. A large number of samples were used to characterize the impact of DEF on concrete properties at different levels of expansion. Chemical tests were performed to observe the initiation and the presence of DEF, while physical and mechanical tests evaluated the impact of DEF on mechanical and transfer properties.

2. Experiments

2.1. Materials

2.1.1. Components

In this study, two cements and two types of aggregates were used. The choice of cements focused on a CEMI and a CEMII, the main characteristics of which are summarized in Table 1. The aggregates used were based on silica or limestone according to the formulations. These two cements have been used in previous studies and show a high swelling potential in the case of DEF, in particular because of their high sulfate, alkali and aluminate contents [8, 11].

Mass content (%)	CEM I 52.5 N	CEMII/A-LL 42.5 R
SiO_2	19.3	19.7
CaO	63.2	63.5
Al_2O_3	5.3	4.6
Fe_2O_3	2.6	3.2
K_2O	0.94	1.36
Na_2O	0.08	0.11
SO_3	3.5	2.7
Total	94.92	95,17

Table 1: Cement composition

2.1.2. Mix designs

The mix designs have already been studied in other experimental works, which make it possible to complete the database on the behavior of these concretes [8, 11]. The first study have highlighted the risk of DEF in these concretes under variable moisture conditions; a decrease of mechanical properties and an increase of transfer properties under DEF degradation have also been shown [8]. Moreover, the impact of accelerating tests method has studied on theses concretes at scale structure, in terms of concrete expansion in [11]. However, some modifications were made in the nature of aggregates used. Indeed, the limestone aggregates used in [8, 11] contain a part of siliceous phase which is not qualified with respect to the risk of Alkali-Silica Reaction (ASR). To avoid a possibly ASR gel formation, the limestone aggregates used in this study is qualified as non-reactive for ASR degradation. The proportion of aggregates was determined with respect to Dreux method in order to reproduce the same aggregate skeleton. The formulations are detailed in Table 2. The CEMII-Si and CEMI-Ca concretes contained siliceous and limestone aggregates, respectively, to show the impact of the nature of aggregates on DEF. The choice of siliceous and limestone aggregates respectively with CEMII and CEMI has been conducted to reproduce mix design representative of nuclear structures. They have also been used for concrete blocks, as part of a new platform test developed by the Radioprotection and Nuclear Safety Institute (IRSN), to study the impact of DEF degradation at scale structure. The concrete casting procedure used in this study followed the protocol of French standards [12, 13].

(a)	CEMII-Si
Material	**Content (kg/m³)**
CEMII/A-LL 42.5 R	350
0/0.315	264
0.315/1	151
1/4	254
4/8	145
8/12	399
12/20	616
Effective water	188
Plasticizer	0,35
Na_2O_{eq}	3,5

(b)	CEMI-Ca
Material	**Content (kg/m³)**
CEM I 52.5 N	400
0/4	718
4/11.2	289
11.2/22.5	813
Effective water	185
Na_2O_{eq}	5

Table 2: Mix designs of "CEMII-Si" (a) and "CEMI-Ca" (b) concrete

2.2. Degradation process

In order to allow rapid development of DEF, IFSTTAR Test N° 66 was adopted, with some modifications [14]. This test comprises four stages: concrete mixing, heat treatment, dry/wet cycles, and final immersion of samples in water at 20°C. The thermal treatment at young age corresponded to that in Al Shamaa's study [8].

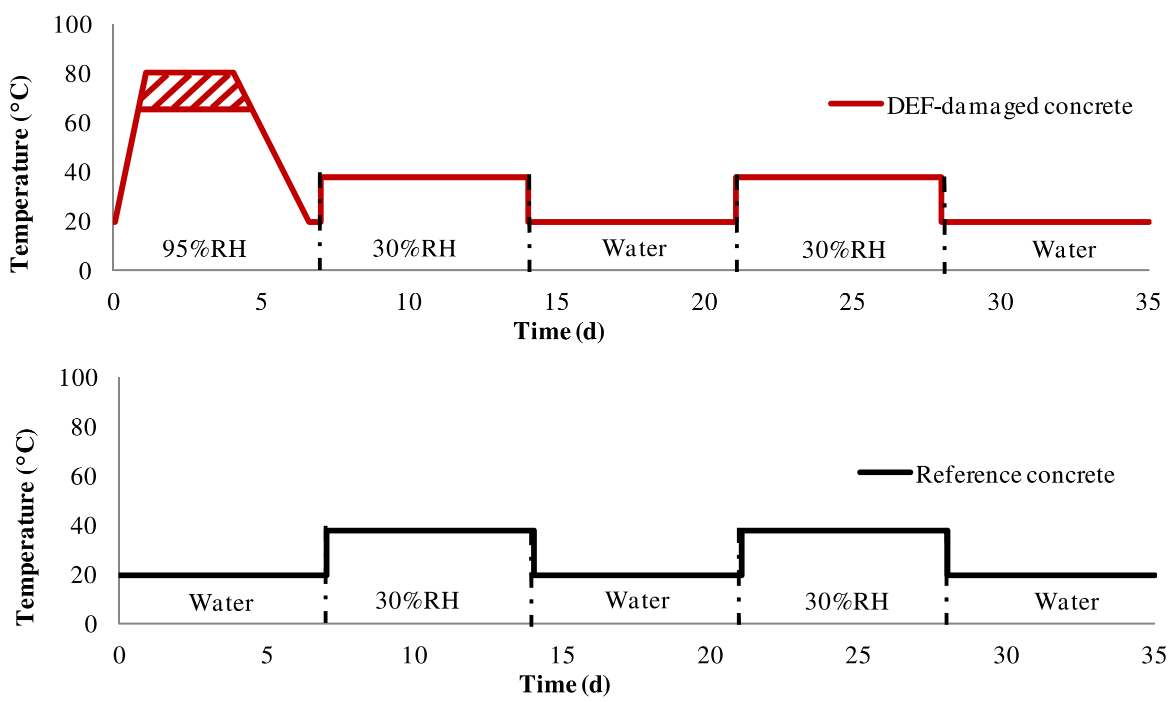

Figure 1: Thermal profile of concretes developing DEF and wet/dry cycles for both concretes

Once cast, specimens were placed in a climate chamber at controlled temperature and relative humidity. The heat treatment was applied for 7 days and comprised four stages: a hold at 20°C, 95% RH for 2h, followed by a rise in temperature from 20°C to 80°C, 95% RH at a rate of 2.5°C/h. Stabilization at 80°C, 95% RH for 72h and a temperature decrease from 80°C to 20°C, 95% RH at a rate of 1°C/h (Figure 1).

As Kchachek and Brunetaud show, the maximum temperature reached in concrete is not the only factor to be taken into account and it cannot be decoupled from the holding time [1,9]. The useful temperature generated by this duration of heat treatment is about 1240°C.h and corresponds to the area under the curve of heat treatment for a temperature above 65°C in Figure 1. The selected dry/wet cycles correspond to the accelerated protocol of IFSTTAR Method N° 66 [15]. They are composed of two 14-day cycles: drying at 38°C, HR < 30% for 7 days and humidification in water at 20°C for 7 days (Figure 1). These cycles allow the initiation of micro-cracking in the concrete and thus accelerate the kinetics of DEF appearance within the concrete without increasing the amplitude of the deformations [2]. The beginning of the degradation is considered to occur at 35 days, at the end of the heat treatment and wet/dry cycles, in this case. During the first 35 days, the concrete is considered to be in a state of hydration where no expansion due to DEF develops. The storage water is not renewed.

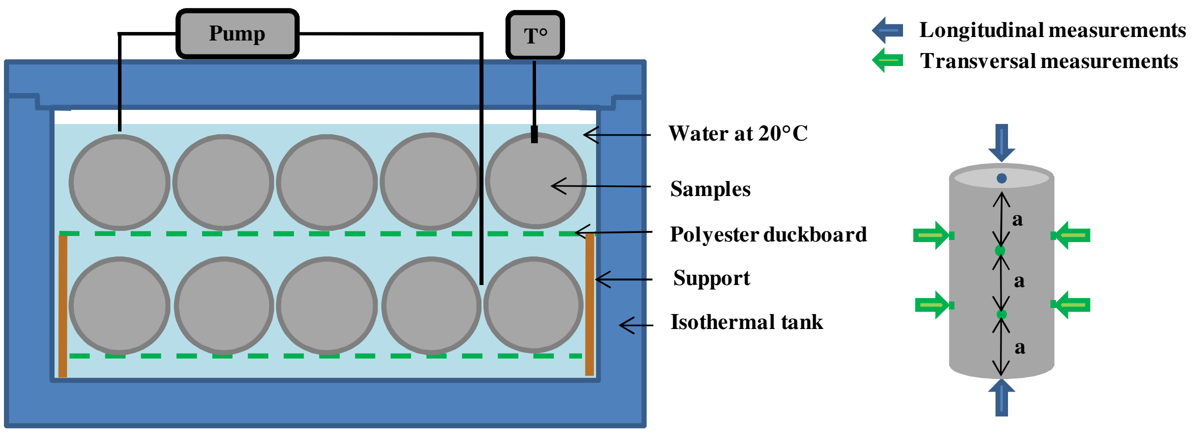

Figure 2: Sample storage and measurements of dimensions

When the wet/dry cycles had been completed, the samples were stored in isothermal containers at 20°C, equipped with a pump to homogenize the temperature and the species present in the water (Figure 2). The reference specimens underwent the same elaboration process but were not subjected to the heat treatment. During the first 7 days, the reference specimens were stored in water at 20°C instead of being heated. Wet/dry cycles were also applied (Figure 1).

The mass and expansion monitoring was performed on three cylindrical test pieces (11 x 22 cm). The shrinkage plots were fixed directly on the mold and were therefore embedded in the concrete. Longitudinal expansion was measured by a digital micrometer having an accuracy of ±1 µm. The transversal expansion was measured by a micrometer having an accuracy of ±5 µm (Figure 2).

2.3. Test protocols

The physicochemical and mechanical tests performed during the experiments are listed in Table 3.

Chemical tests	**Physical tests**	**Mechanical tests**
pH of pore solution	Electrical resistivity	Compressive strength
Portlandite content	Chloride migration	Static moduli
SEM observation	Water porosity	Dynamic moduli
Alkali content	Gas permeability	

Table 3: Physicochemical and mechanical tests performed during the experiments

In order to observe the evolution of the physicochemical and mechanical properties of concrete during its degradation by DEF, chemical analyses were performed to ensure the presence of pathologies in the concrete. When the pathology was initiated (expansion of 0.04%), measurement of the physical properties revealed the impact of the micro-cracking generated on the transfer properties. Finally, measuring the mechanical properties gave some indications on the state of damage of the concrete subjected to these pathologies. Measurements of all the properties were made at the different degrees of expansion shown in Figure 3. The expansion curve due to DEF can usually been described as a sigmoid (Fig. 3), with three phases:

- The latent period is characterized by the precipitation of DEF in the microstructure (Porosity, Interface Transition Zone (ITZ), Hadley grain) [1]. Expansion is small in this period. When the tensile strength of concrete is reached due to internal pressure, cracks were generated.

- The precipitation of DEF in cracks, leads to cracks propagation and so to the acceleration of expansion.

- Finally, the deceleration of swelling occurs when one reactant is consumed and/or when the cracks opening is sufficiently significant to accommodate new products without generation of supplementary expansion [1].

In order to detect the presence of DEF, the first characterization was conducted after curing in the initial state, at 35 days. When swelling begins, during the latent period, two characterizations were performed. Two other measurements were carried out during the acceleration phase and a final characterization was performed during the stabilization period.

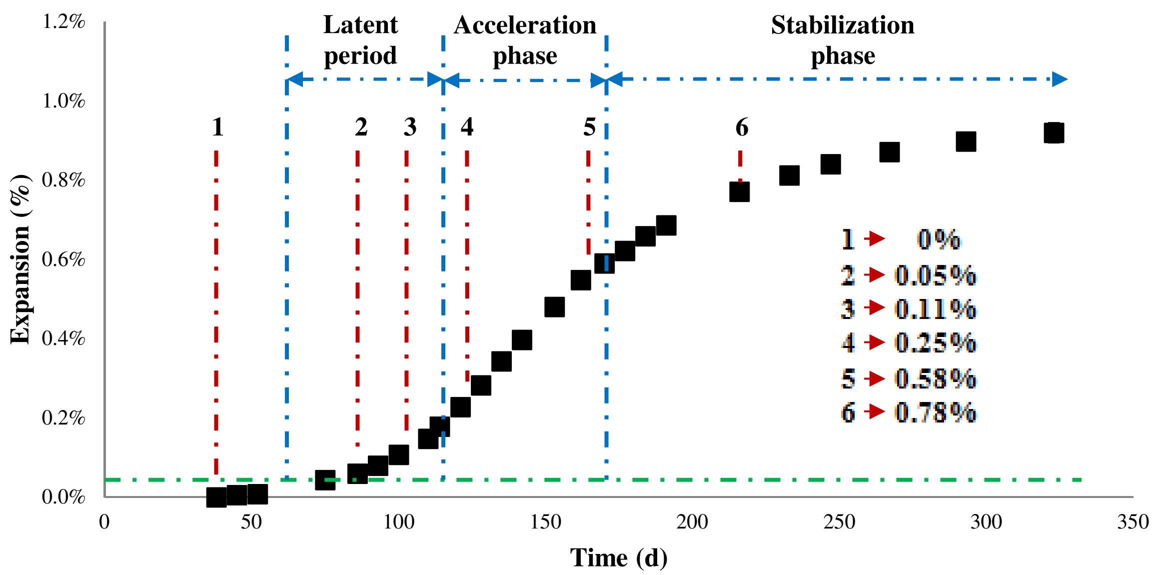

Figure 3: The 6 levels of expansion for the measurement of properties

2.3.2. Chemical tests

Two chemical tests were performed: pH measurement and determination of portlandite content.

The pH measurement was carried out on an 11 x 22 cm cylindrical specimen. The test piece was broken in compression. The pieces present in the center of the specimen were placed in a press to extract the interstitial solution present in the concrete. The pH was measured by a probe. The pore solution was then stabilized by acid and analyzed by Inductively Coupled Plasma Mass Spectrometry (ICP-MS) to determine the elements and their amounts.

The portlandite content was experimentally determined by Thermo-Gravimetric Analysis (TGA) on a sample taken from an 11 x 22 cm cylindrical specimen. The central part of the test piece was broken into small pieces and dried in a lyophilizer for 1 day. This part was then polished and metallized for Scanning Electron Microscopy (SEM) observation to check that DEF was present in the concrete.

2.3.2. Physical tests

Four physical tests were performed: electrical resistivity, chloride migration, porosity measurements, and gas permeability.

The electrical resistivity and non steady state chloride migration tests were performed according to the standard, on the same three 11 x 5 cm cylindrical samples obtained from an 11 x 22 cm one [15,16]. The saturated concrete solution of the tests was replaced by a NaOH concentration of 0.1 mol/l according to a new test protocol (PerfDub).

Gas permeability and water porosity tests were performed according to the standards [17, 18]. However, the drying temperature has been adopted at 40°C for two reasons: this helps to avoid the destabilization of the delayed ettringite formed during the development of ISR and on the other hand allows limiting the additional cracking caused by drying to 105°C, proposed in the standards. In this case, the evolution of gas permeability during the expansion will mainly due to concrete DEF damage by limiting supplementary cracks due to high drying temperature.

2.3.1. Mechanical tests

Three mechanical properties were measured: the compressive strength, and the static and the dynamic moduli. Linear and nonlinear acoustic methods were employed to determine the dynamic moduli.

Compressive strength and static moduli were measured on three 11 x 22 cm cylindrical specimens according to the standards [19, 20].

Several tests in development to determine the dynamic moduli are presented in the literature. These tests have already been performed in the case of DEF damage [1, 8]. In this study, the dynamic moduli was determined by two measurements. Linear acoustic emission was performed in transmission and reception on the same specimens. The equipment used included a SOFRANEL 5077PR signal generator, a TEKTRONIX oscilloscope and 250 kHz longitudinal and transversal wave transducers. To improve the signal quality, a viscous liquid was needed at the concrete/transducer interface; in this test, honey was used. The dynamic moduli was determined from equation 1:

$$E_{dyn} = \rho.V_t^2.\left(\frac{3.V_l^2-4.V_t^2}{V_l^2-V_t^2}\right) \qquad (1)$$

with E_{dyn} the dynamic moduli (Pa), ρ the density in kg/m^3, V_t the shear wave velocity (m/s), V_l the compression wave velocity (m/s).

A nonlinear acoustic emission method was also used to evaluate the dynamic moduli. The principle is to generate a pulse at the base of the test piece using a hammer. The resonance of the specimen generates a signal collected by an accelerometer on the other side of the specimen and treatment of the signal by a Fourier transformation gives the natural frequency of longitudinal resonance of the material. The moduli is then determined by equation 2:

$$f_{long} = \frac{1}{2L}\sqrt{\frac{E_{dyn}}{\rho}} \qquad (2)$$

with L the specimen length (m) and f_{long} the longitudinal natural frequency of the material (Hz).

3. Experimental results

3.1. Expansion

Figure 4a shows the evolution of expansion as a function of time for the CEMII-Si and CEMI-Ca concretes and their corresponding references CEMII-Si-ref and CEMI-Ca-ref. IFSTTAR method n° 66 refers to a swelling limit of 0.04% in an expansion test [14]. Beyond this threshold, there is a risk of the concrete being damaged by DEF. The reference formulations did not exceed the limit threshold and showed a maximum swelling of 0.02%.

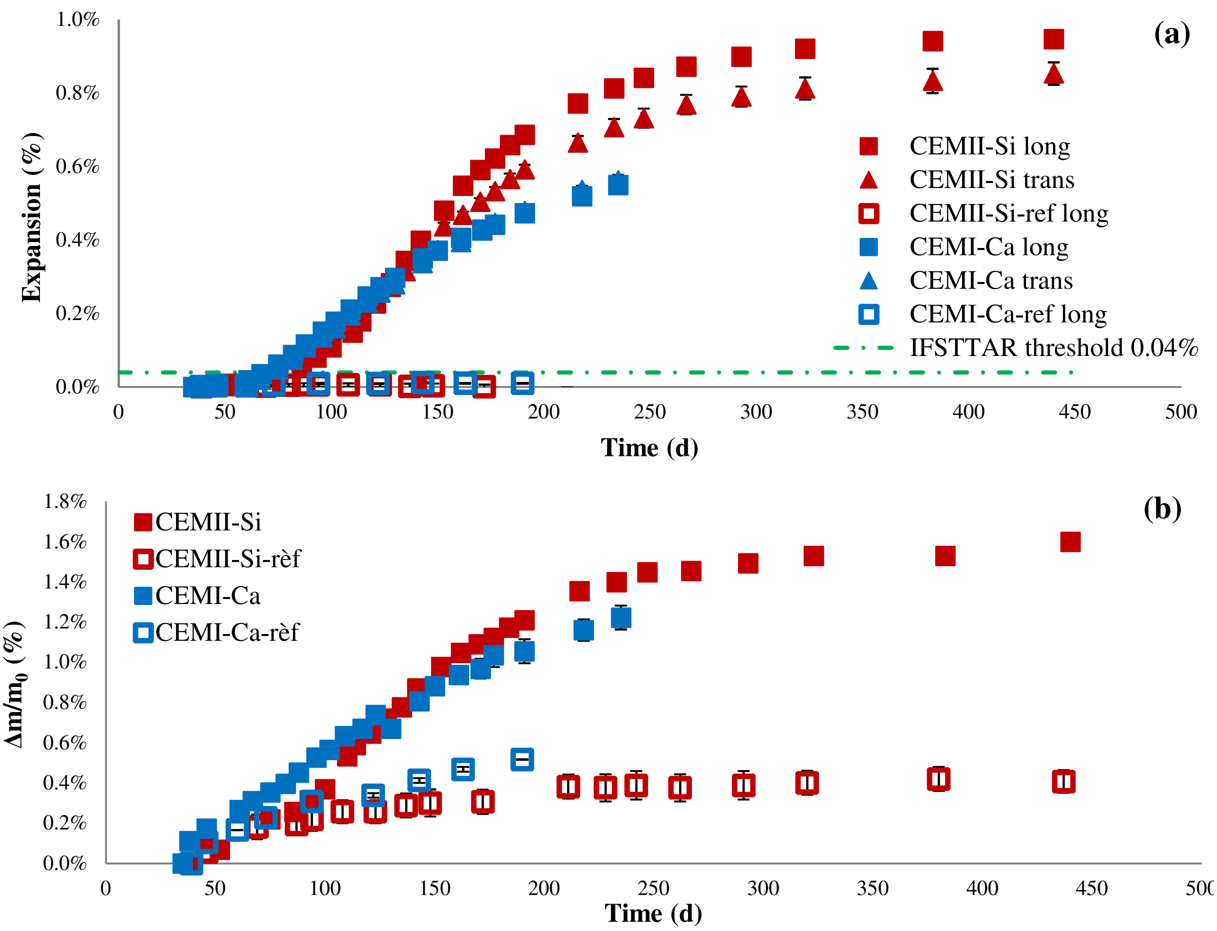

Figure 4: Evolution of expansion (transversal and longitudinal) (a) and mass gain (b) versus time

Specimens developing DEF showed significant swelling, around 0.9%, at the end of the expansion for CEMII-Si. The latent period began at around 70 days, or 35 days after curing. For the CEMI-Ca design, this period started at 60 days and ended quickly. The first point of inflection was at 80 days for the CEMI-Ca and 110 days for the CEMII-Si concrete. CEMI-Ca contained large limestone aggregates that lead to a decrease of the latent period [21]. This phenomenon is attributed to the higher bonding in case of limestone aggregates with the cement matrix. In this case, cracks generated at the ITZ during the heat treatment due to a differential dilatation coefficient between paste and aggregates, were reduced [21]. On the one hand, the low cracking results in a lower volume available to accommodate the new phases due to DEF without inducing cracking and expansion. On the other hand, the low cracking leads to a decrease of transfers properties in concrete and thus to delay DEF expansion. These two phenomena are opposed. Indeed, a decrease in transfer properties cannot explain the lowest latency period observed in the case of limestone aggregates. The decrease in available volume caused by the low cracking at the ITZ therefore seems to be the cause of the decrease in latency period. In this case, the volume of DEF necessary to generate pressure is reduced and it leads to a decrease of latent period.

The final expansion of CEMI-Ca showed a swelling of around 0.6%. This lower swelling was attributed to the presence of limestone aggregates, which allowed the bond between aggregate and cement paste to be increased by the formation of calcium hydrates around the aggregates and equally due to a high mechanical interlocking behavior [5, 22, 23, 24]. The cracks generated by DEF at the ITZ were also reduced, allowing a lower final expansion [5, 23].

Figure 4b shows the evolution of mass as a function of time. The initial mass, m_o, was measured at 35 days. Reference samples have a mass gain of 0.4% stabilizing around 200 days. This increase was due to their storage in water at 20°C. For CEMII-Si and CEMI-Ca concretes, the mass increase was proportional to the swelling of the concrete. In addition, the kinetics of the mass gain for these two pathological concrete was in agreement with the kinetics of swelling, which confirms the short latent period in the CEMI-Ca specimens (Figure 4a). The mass gain of CEMII-Si and CEMI-Ca concrete reached respectively 1.5 and 1.2% at the end of expansion.

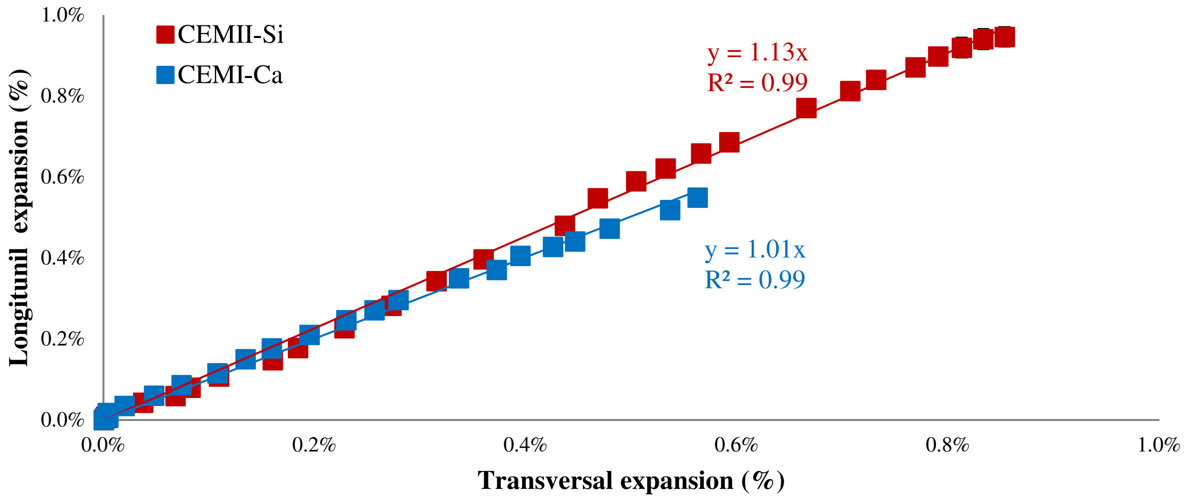

Figure 5: Evolution of longitudinal vs. transversal expansion

The longitudinal and transversal expansion measurements reported in Figure 5 are proportional. The slope of proportionality is equal to 1, confirming the isotropy of the swelling already observed in stress free conditions [25]. However, the transversal swelling is slightly lower on the CEMII-Si concrete at the end of expansion.

3.2. Microstructure evolution

The presence of delayed ettringite was observed by SEM for each degree of expansion.

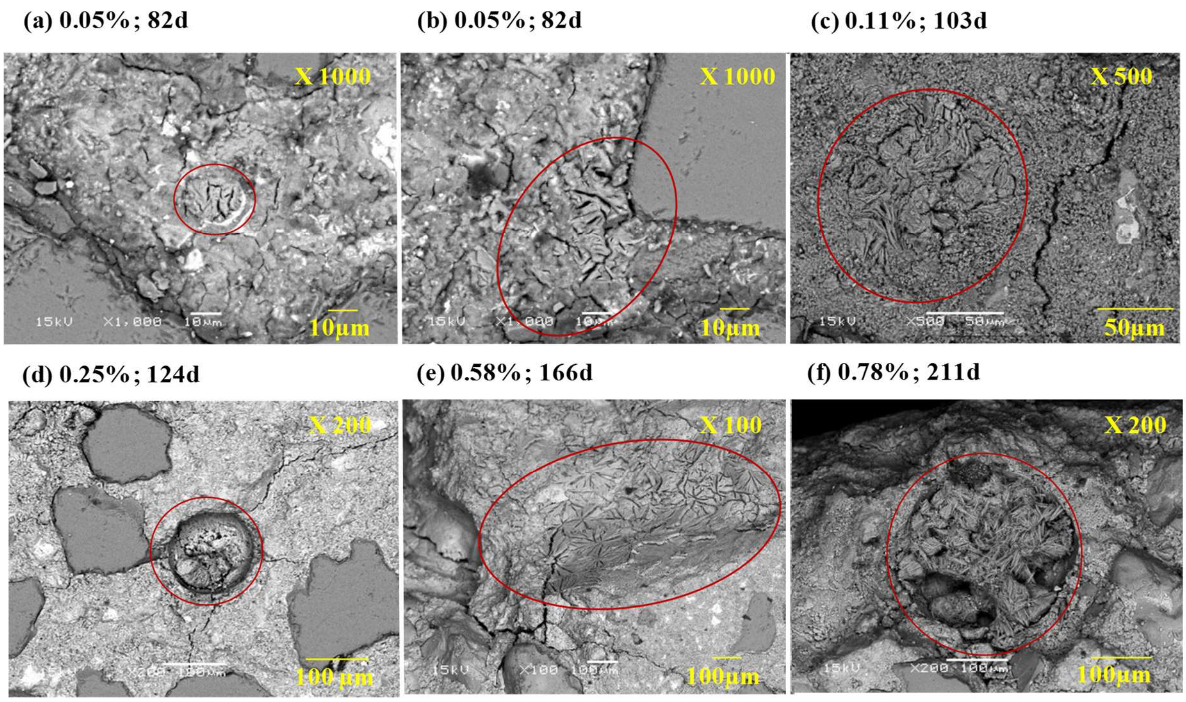

Figure 6: SEM images of the CEMII-Si concrete

Figure 6 shows the presence of delayed ettringite in massive and compressed form for different degrees of swelling. In the CEMII-Si formulation, siliceous aggregates were used. The SEM images show that the initiation of swelling was induced by the formation of delayed ettringite in Hadley grains (Figure 6a) and at the ITZ (Figure 6b). The swelling measured at this degree was 0.05%. As expansion continued, delayed ettringite continued to develop in these areas and in the porosity (Figure 6c and 6d). Then there was a separation from the cement paste all around the aggregates (Figure 6d). At the time corresponding to 0.25% of swelling, the cracks propagated from this interface to the porosity, causing an acceleration of swelling. When expansion continued, the presence of delayed ettringite became increasingly significant, both in the cement paste (Figure 6e) and in the porosity (Figure 6f).

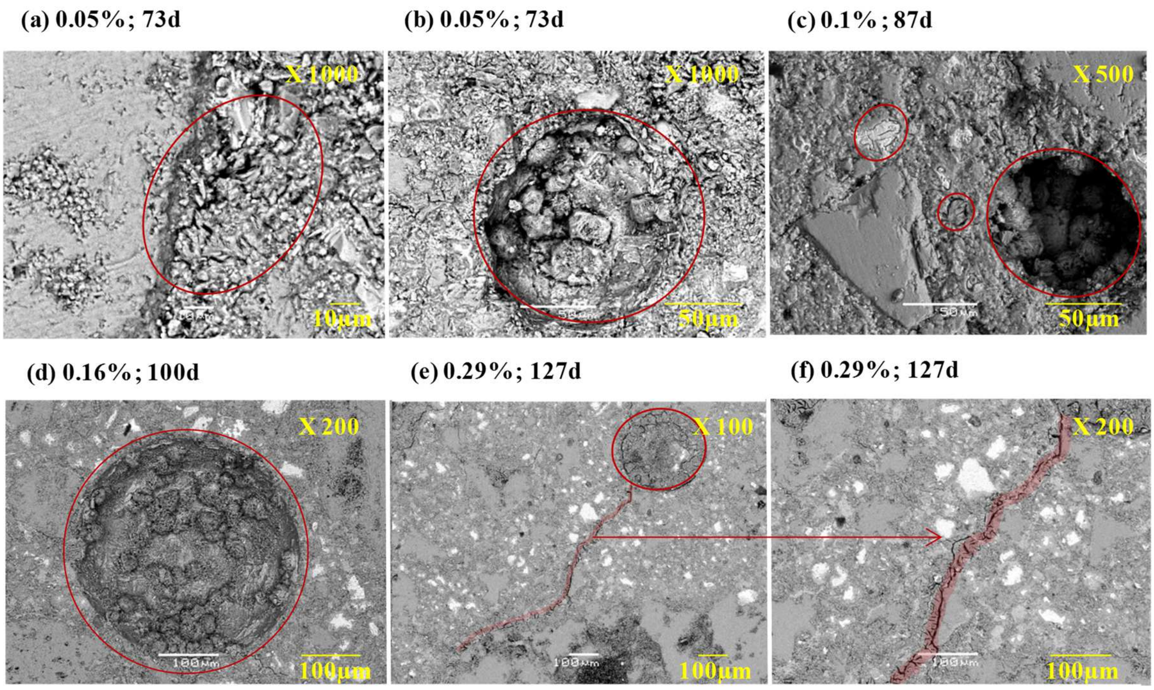

Figure 7: SEM images of the CEMI-Ca concrete

The SEM observations on the CEMI-Ca were consistent with those observed on the CEMII-Si concrete as ettringite developed primarily at the ITZ, in the Hadley grains and in the porosity (Figures 7a and 7b). As expansion continued, delayed ettringite continued to propagate in these areas (Figures 7c and 7d). When these preferential zones began to be completely filled by ettringite, the cracking propagated between them (Figures 7e and 7f) and the ettringite gradually began to fill the generated cracking. This step marked the acceleration of the degradation. However, cracking generated at the ITZ in the case of limestone aggregates did not propagate all around the aggregate, thus confirming the observations of Yang et al. [23].

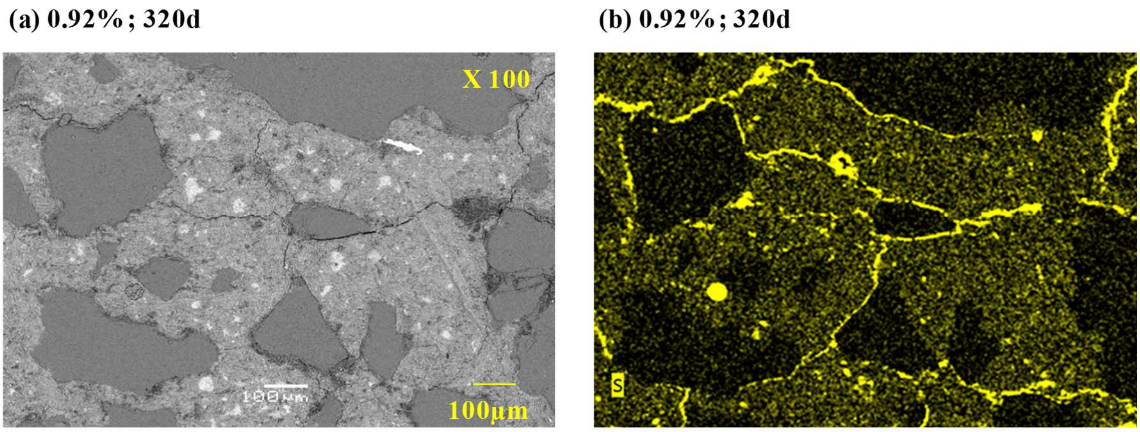

Figure 8: CEMII-Si SEM images (a) initial image and (b) sulfur image (mapping)

These results show that, for each formulation, the presence of delayed ettringite is found first at the ITZ in the Hadley grains and in the porosity. Ettringite then propagates in and between these preferential zones, generating more and more cracking. This cracking marks the acceleration of the expansion. As mentioned above, the cracking generated at the ITZ depends on the nature of the aggregates [23]. In the case of siliceous aggregates, cracking is generated all around the aggregate but it only partially surrounds limestone aggregates. Ettringite then spreads in existing fissures. Figure 8b shows the presence of sulfur in the sample (yellow in Figure 8b), proving the presence of delayed ettringite in concrete cracks. These observations confirm that the cracks caused by the pathology are filled with ettringite during the expansion. Recently, Brunetaud [1] had proposed a global swelling theory to explain the DEF propagation. This theory is based on a homogeneous swelling of concrete. Delayed ettringite would initially form in Hadley grains and porosity. The pressure generated by the DEF in the cement matrix would lead to the presence of cracks at the ITZ (rigid inclusion) and the development of delayed ettringite in this area. The crystallization pressure generated by the formation of ettringite in these areas would lead to cracks propagation and thus accelerate the degradation. These results are in agreement with this theory: delayed ettringite was first observed in the Hadley grain, in the porosity and at the ITZ. Then delayed ettringite was observed in the cracks.

3.3. Detection criterion

The first aim of this experimental work was to find a very sensitive test allowing DEF detection. DEF can be detected if the evolution of one of the properties measured in this work is significant (sufficiently higher than the scatter on results) and only due to DEF expansion (not to concrete hydration). In this aim, a DEF detection criterion for physicomechanical properties was developed, taking the effect of hydration and experimental scatter into account (equation 3).

$$X_{i\, threshold}(t) = X_0\left(1 + \frac{X_{i\, ref}(t) - X_{0\, ref}}{X_{0\, ref}}\right) \pm 2\overline{\sigma_{ref}} \qquad (3)$$

with $X_{i\ threshold}(t)$ the threshold value of detection of the property measured in time, X_0 the initial value of the pathological concrete, $X_{0\ ref}$ the initial value of the reference concrete, $X_{i\ ref}(t)$ the value of the property of the reference concrete in time and $\overline{\sigma_{ref}}$ the average of the standard deviations obtained on the reference specimens.

For the measurement of the chemical properties, the high dispersion of results did not allow this criterion to be used.

3.4. Chemical properties

3.4.1 pH measurement and portlandite content

The pH analysis of the interstitial solution was performed for different degrees of expansion. Figure 9a shows the evolution of the pH for the CEMII-Si and CEMI-Ca concretes and Table 4a summarizes the pH results obtained on the reference concretes. No significant change in the pH was observed on the reference specimens or on those developing the pathology (Table 4a and Figure 9a). The pH of the interstitial solution of CEMII-Si concrete remained stable at a value of approximately 13.3 and that of the CEMI-Ca was also stable during the expansion, at around 13.4. The associated reference specimens showed the same trends, with pH around 13.4 for CEMII-Si-ref and around 13.5 for CEMI-Ca-ref.

(a)	35d	90d	180d
CEMII-Si-ref	13.5	13.3	13.4
CEMI-Ca-ref	-	13.7	13.3

(b) (wt.%)	35d	90d	180d
CEMII-Si-ref	13.4	11.9	11.4
CEMI-Ca-ref	15.7	15.9	17.3

Table 4: pH (a) and portlandite (b) evolution over time for reference concretes

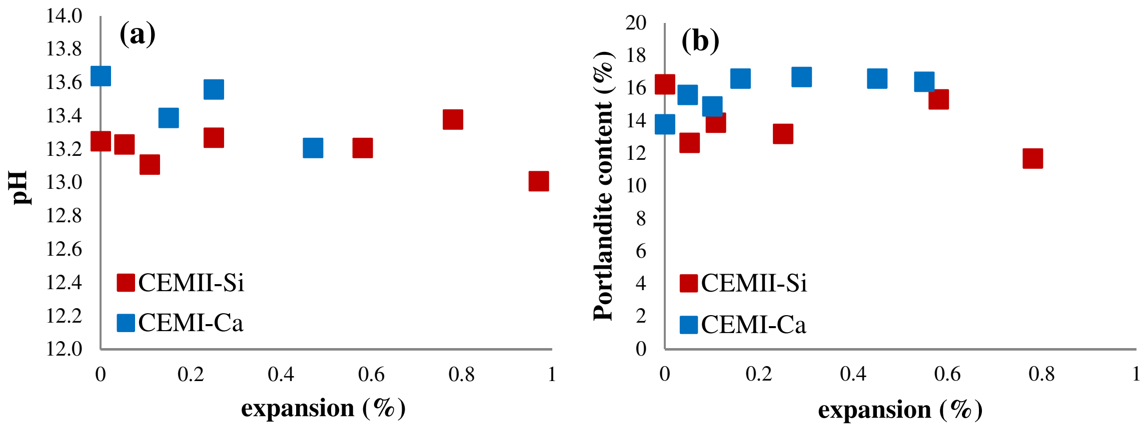

Figure 9: pH (a) and portlandite (b) evolution versus expansion for concretes damaged by DEF

The leaching of alkalis should have lowered the pH to about 12.6 over time, due to portlandite pH buffering [26]. The test protocol may have been partly responsible for these stable, high pH values. Chappex and Scrivener observed an increase in alkali concentrations in accordance with the pressure applied up to 800 MPa [27]. During the present test, the pressure was about 900 MPa. It is possible that the alkalis adsorbed physically on the surface of the hydrates were released into the solution, leading to a pH buffering.

The evaluation of portlandite content performed by ATG on concrete samples (Figure 9b) shows that it remained stable during the degradation, at between 11 and 17% for all concretes. The oscillation of the values was a consequence of the sample used. This test is usually performed on cement paste.

X-Ray Diffraction (XRD) analyses were conducted on the same samples. During the degradation, no new formed phase was observed. The delayed ettringite being poorly crystallized, its presence was not detected. In addition, the large peaks of calcite or silica, depending on the nature of the aggregates used, masked the hydrated phases, thus making the analysis complex.

3.4.2 Alkali concentrations

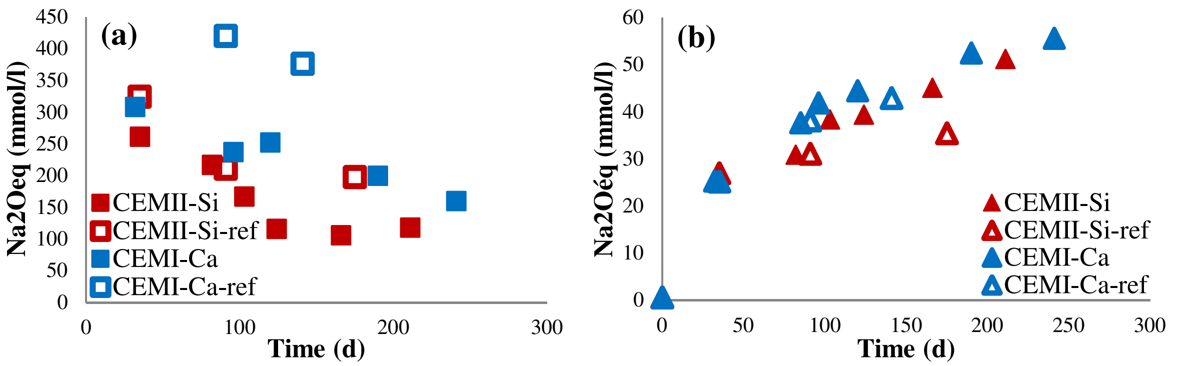

Figure 10: Evolution of the equivalent alkali content in the interstitial solution (a) and in the storage water (b) versus time

Figures 10a and 10b represent the evolution of the equivalent alkali content, expressed in mmol/l, contained in the interstitial solution and in the storage water, respectively, for each concrete. Figure 10b shows the strong leaching of alkali during the first 35 days. In fact, the initial Na_2O_{eq} concentration of the storage water was 0.6 mmol/l. At 35 days, this water contained a concentration of 25 mmol/l. This significant leaching came, in particular, from the fact that micro-cracking was generated during the wet/dry cycles. Underwater storage, resulting in alkali leaching, continued over time. However, the leaching of specimens developing the pathology seems to be greater than that of the reference concretes. At 200 days, the storage water of concretes developing DEF was found to have a concentration of 50 mmol/l, against about 40 mmol/l for reference concretes. This supplement of leaching can be attributed to micro-cracking in the material, generated by the swelling of DEF.

Figure 10a confirms these results. The alkali leaching of interstitial water is greater for the pathological concretes. In addition, the concentration of Na_2O_{eq} of the reference concretes seems to stabilize after 100 days. This stabilization could be attributed to the filling of the pores at the periphery of the test piece with calcite. This phenomenon has also been observed and discussed by Thibaut [28]. However, although the initial amount of alkali in the CEMI-Ca and CEMI-Ca-ref concretes was higher, the leaching generated during the first 35 days significantly decreased their concentration. The Na_2O_{eq} concentration of the CEMI-Ca and CEMII-Si concretes was found to be close respectively 308 and 261 mmol/l at 35 days despite the difference of alkali content in the initial state.

The measurement of the portlandite content and the pH of the interstitial solution showed no evolution during the degradation. The significant leaching of alkali over time was mainly due to the storage. These chemical properties do not make it possible to detect DEF during the degradation.

3.5. Physical properties

3.5.1. Chloride migration

Non steady state chloride migration tests and electrical resistivity measurements were performed on the same test specimens. Figure 11 shows the evolution of the chloride migration coefficient as a function of the expansion generated by the pathology. The CEMII-Si-ref and CEMI-Ca-ref references had a migration coefficient that hardly varied over time (by 13×10^{-12} and 11×10^{-12} m² respectively (Table 5)).

($\times 10^{-12}$ m²)	35d	90d	180d
CEMII-Si-ref	**12.6 ±0.2**	**12.8 ±0.3**	**14.9 ±1.8**
CEMI-Ca-ref	**10.3 ±0.4**	**11.2 ±0.3**	**10.2 ±1.1**

Table 5: Evolution of the coefficient of migration of chlorine ions according to time for reference concretes

Concretes developing pathology had a higher migration coefficient, around 30×10^{-12} m², before DEF expansion. There are several reasons to believe that this increase in comparison with the reference concrete was due to the heat treatment effect. The heat treatment may have generated a modification of the composition of the cement paste and the hydrates formed [29]. In addition, the thermal expansion effects may have damaged the cement paste and the ITZ [21, 30].

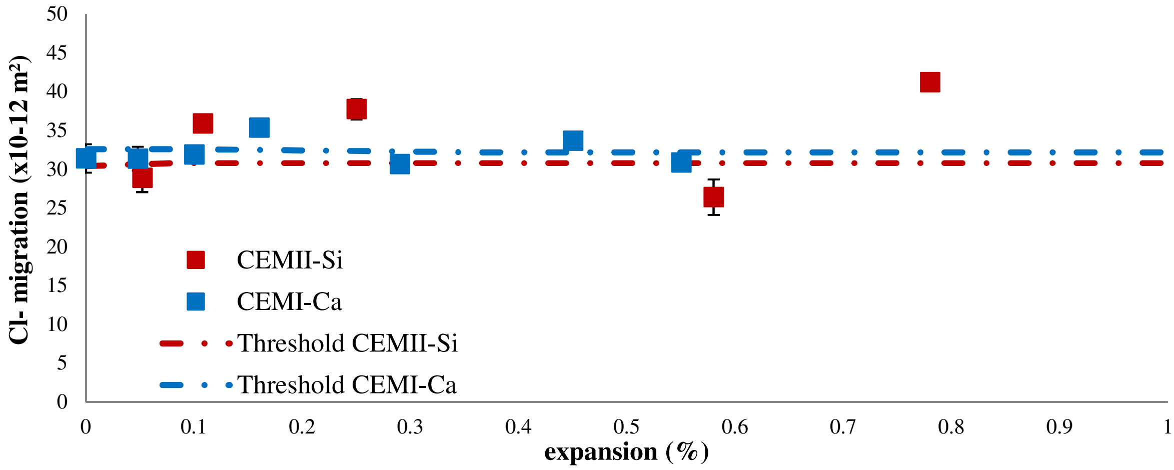

Figure 11: Evolution of the coefficient of migration of chlorine ions according to the expansion for concretes damaged by DEF

For the concretes developing the pathology, no significant increase in the migration coefficient was observed. This phenomenon can be explained by the fact that the chloride ions diffused uniformly in the cement paste through the porosity and micro-cracking due to DEF after expansion. When measurements were taken, this generated a linear penetration front despite the presence of macro-cracking. The wide scatter of the results did not allow the detection of DEF.

3.5.2. Electrical resistivity

The electric resistivity tests (Figure 12) showed greater sensitivity. Reference concretes CEMII-Si-ref and CEMI-Ca-ref had a resistivity of 45 Ω.m at 35 days (Table 6). The concretes developing the pathology had a lower resistivity, around 35 Ω.m, at the same time, the heat treatment having caused additional damage.

(Ω.m)	35d	90d	180d
CEMII-Si-ref	**45.0 ±2.2**	**55.0 ±3.8**	**58.0 ±4.9**
CEMI-Ca-ref	**45.0 ±1.0**	**51.0 ±1.7**	**55.0 ±4.0**

Table 6: Evolution of the electrical resistivity over time for reference concretes

In Figure 12, a gradual decrease in the resistivity is observed during the degradation for each pathological concrete. A threshold of around 25 Ω.m is reached at 0.3% expansion. This threshold of resistivity could be due to the cracking caused by the pathology being gradually filled by ettringite. In contrast, for the reference concretes, the electrical resistivity increased significantly between 35 and 90 days. A resistivity gain of 25% was observed from day 35 to day 180, due to the continuation of the hydration reactions causing a densification of the concrete.

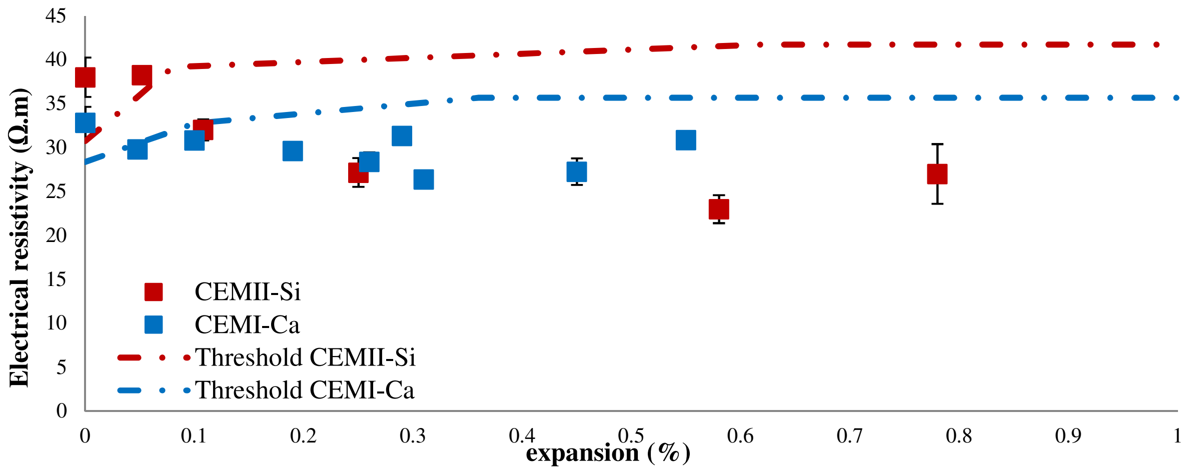

Figure 12: Evolution of the coefficient of the electrical resistivity according to the expansion for concretes damaged by DEF

With the chosen criterion (Eq. 3), the detection of DEF took place between 0.05 and 0.1% of expansion, during the latent period. Between these two expansion levels, the decrease of resistivity was sufficient to point out significant damage.

3.5.3. Water porosity

Figure 13 shows the evolution of the water-accessible porosity as a function of the expansion caused by DEF. The reference concretes CEMII-Si-ref and CEMI-Ca-ref show no evolution over time despite the continuation of hydration reactions (Table 7).

(%)	35d	90d	180d
CEMII-Si-ref	**11.2 ±0.7**	**11.4 ±0.2**	**11.9 ±0.3**
CEMI-Ca-ref	**12.8 ±0.3**	**13.4 ±0.4**	**13.7 ±0.3**

Table 7: Evolution of water porosity over time for reference concretes

The porosity measured on the CEMII-Si concrete remains lower than that measured on the CEMI-Ca concrete. The use of limestone aggregates of higher porosity for CEMI-Ca concretes could explain this difference, the water absorption coefficient of these aggregates being greater: 2.6% against 0.6%. When the concrete is damaged by delayed ettringite formation, porosity tends to increase, this being attributed to the formation of a crack network, filled by water. The increase in porosity is rapid at the beginning of the expansion and then stabilizes at the end of the expansion period. This stabilization can be explained by a competition between crack opening and crack filling with delayed ettringite.

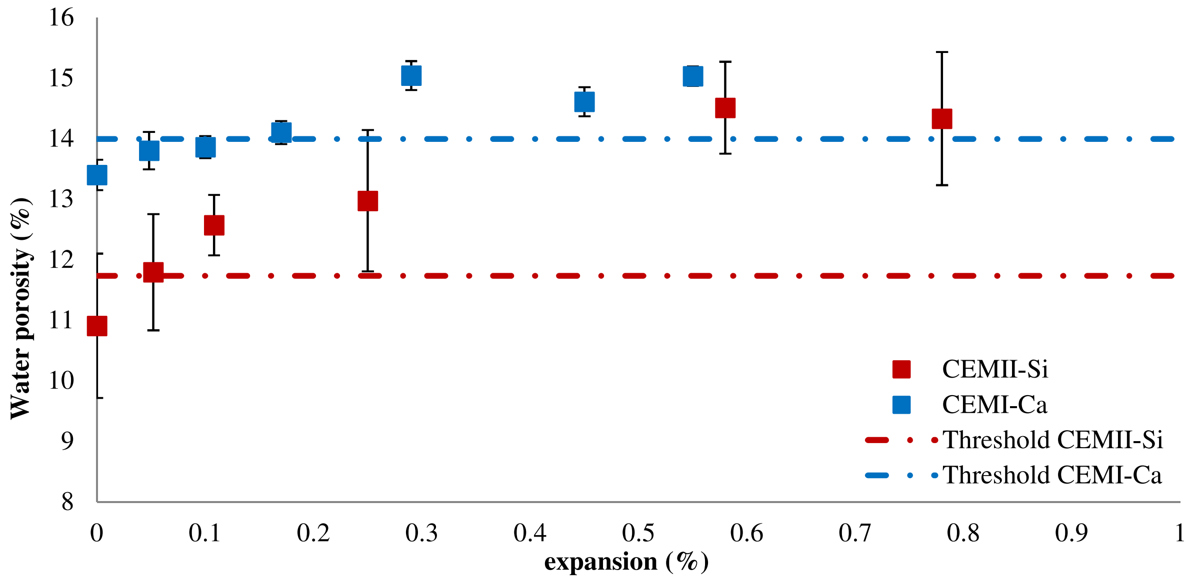

Figure 13: Evolution of water porosity as a function of expansion for concretes damaged by DEF

Depending on the criterion chosen, the detection takes place between 0.15 and 0.25% of expansion, at the beginning of the acceleration phase.

3.5.4. Gas permeability

Figure 14 shows the evolution of the apparent air permeability coefficient according to the expansion generated by DEF. The reference concretes CEMII-Si-ref and CEMI-Ca-ref show no change in their coefficients of permeability over time of 110×10^{-18} m² (Table 8).

($\times 10^{-18}$ m²)	**35d**	**90d**	**180d**
CEMII-Si-ref	**110 ±23**	**106 ±12**	**101 ±27**
CEMI-Ca-ref	**101 ±38**	**111 ±13**	**120 ±10**

Table 8: Evolution of apparent gas permeability coefficient over time for reference concretes

The CEMII-Si and CEMI-Ca concretes developing the pathology have apparent gas permeability coefficients that are similar, respectively equal to 125×10^{-18} m² and 60×10^{-18} m² before expansion. During expansion, the CEMII-Si concrete shows a strong increase in the coefficient of permeability at the beginning of expansion (permeability at 0.05% is double that before expansion). The CEMI-Ca also shows an increase but it occurs later and is smaller. This difference could be due to the mineralogical nature of the aggregates used. The ITZ of concretes containing limestone aggregates seems to be improved [5, 22, 23]. As mentioned above, cracks due to DEF passing through this interface are reduced in the case of limestone aggregates [23]. There may be fewer preferential paths in the CEMI-Ca concrete, causing a smaller increase in the coefficient of permeability at early expansion. When the acceleration phase of the pathology is reached, at around 0.2% of swelling, the permeability is significantly impacted. This drastic increase can be attributed to the formation of more and more percolating paths within the material, generating a large increase of gas flow during the test. These results are therefore in agreement with those of Al Shamaa et al. [31].

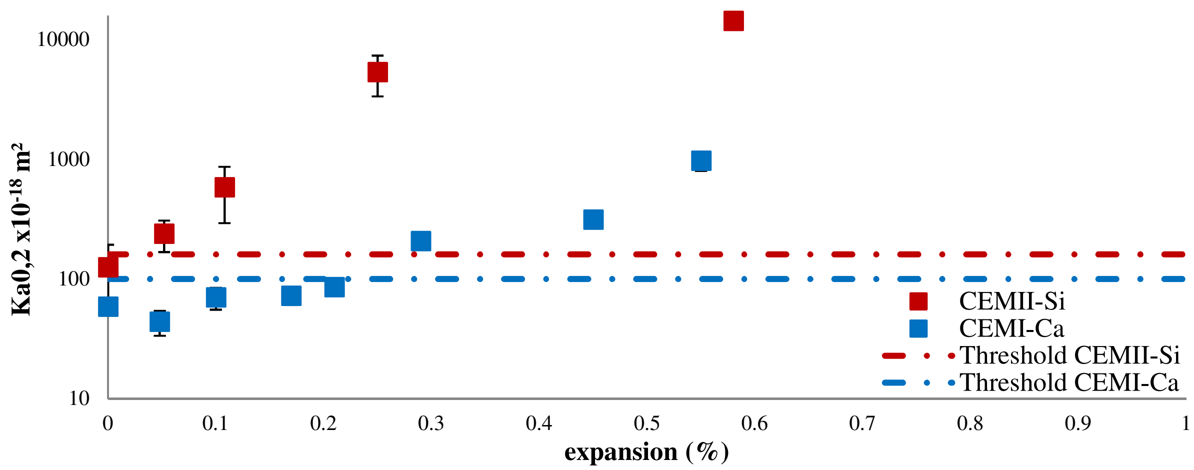

Figure 14: Evolution of apparent gas permeability coefficient according to the expansion for concretes damaged by DEF

Depending on the criterion chosen, the detection takes place during the latent period before 0.05% expansion for CEMII-Si concrete and at the beginning of the acceleration phase, between 0.17 and 0.29%, for CEMI-Ca concrete.

3.6. Mechanical properties

3.6.1 Compressive strength

The compressive strength measurements also show the impact of the heat treatment on the mechanical properties. The reference concretes CEMII-Si-ref and CEMI-Ca-ref have compressive strengths of 34 MPa and 44 MPa, respectively, at 35 days (Table 9).

(MPa)	35d	90d	180d
CEMII-Si-ref	**34.0 ±2.0**	**34.1 ±1.3**	**38.3 ±0.5**
CEMI-Ca-ref	**43.5 ±1.5**	**48.2 ±1,4**	**49.0 ±0.3**

Table 9: Evolution of the compressive strength over time for reference concretes

The compressive strengths of CEMII-Si and CEMI-Ca are lower, at 23 MPa and 29 MPa, respectively. The reduction of the compressive strength by the heat treatment can be explained as previously by the occurrence of damage in the cement paste and the ITZ and by the modification of the composition of hydrates [21, 29, 30]. The compressive strength of CEMI-Ca and CEMI-Ca-ref concretes remains higher than those of other concretes and increases with time following the hydration process. This difference is explained by the fact that these concretes contain a larger amount of cement and a lower W/C ratio, and also because the presence of limestone aggregates in the formulation improves the ITZ. The CEMII-Si and CEMI-Ca pathological concretes show compressive strength that remains stable during the initiation of the pathology. However, during the acceleration phase, the strength decreases spontaneously and then stabilizes at the end of the acceleration period. These results are in accordance with those of Bouzabata et al. [25]. The compressive strength drop is 30% and 20% for the CEMII-Si and CEMI-Ca concretes, respectively, at the middle of expansion.

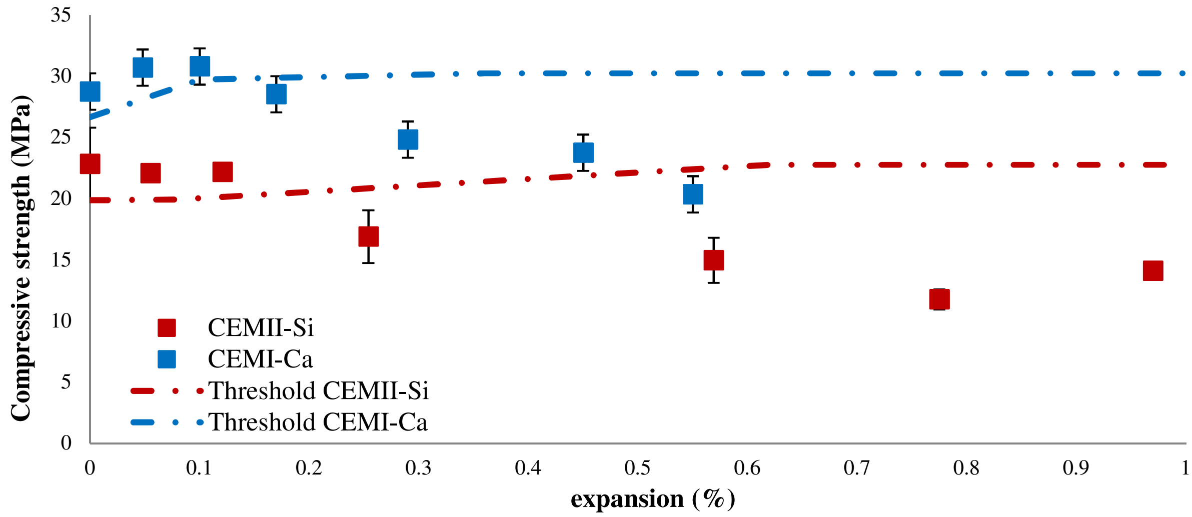

Figure 15: Evolution of the compressive strength according to the expansion for concretes damaged by DEF

Depending on the criterion chosen, the detection takes place between 0.17 and 0.25% of expansion, at the beginning of the acceleration phase.

3.6.2 Static moduli

The static moduli of CEMII-Si-ref and CEMI-Ca-ref reference concretes shows small changes between 35 and 190 days (Table 10). The moduli is still higher for CEMII-Si-ref concrete (equal to 40 GPa) than for CEMI-Ca-ref concrete (31 GPa) at 35 days.

(GPa)	35d	90d	180d
CEMII-Si-ref	**40.4 ±2.5**	**39.4 ±0.4**	**43.3 ±1.0**
CEMI-Ca-ref	**31.9 ±0.01**	**32.1 ±0.5**	**33.0 ±0.5**

Table 10: Evolution of the static moduli as a function of time for reference concretes

However, the CEMII-Si and CEMI-Ca pathological concretes reveal that the moduli decreases progressively during the expansion. A significant decrease in the moduli is observed for swelling of around 0.2% during the acceleration phase of the pathology (Figure 16). At this time, the moduli decreases by 40% and 50% for the CEMII-Ca and CEMII-Ca-ref concretes, respectively. The loss of static moduli seems to be proportional to the expansion rate caused by the pathology. These results are not in agreement with those of Al Shamaa et al., who show no decrease of static moduli during the latent period [10].

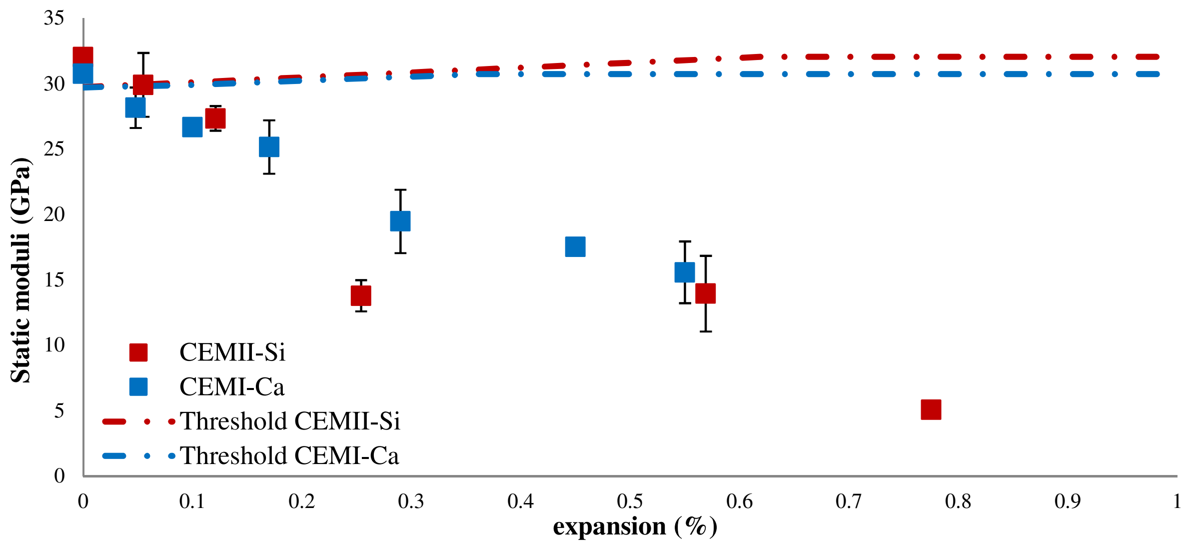

Figure 16: Evolution of the static moduli according to the expansion for concretes damaged by DEF

Depending on the criterion chosen, the detection takes place between 0.05 and 0.1% of expansion, during the latent period.

3.6.3 Dynamic moduli

Figure 17a shows the evolution of the dynamic linear acoustic moduli according to expansion. The reference concretes CEMII-Si-ref and CEMI-Ca-ref show no moduli evolution over time (moduli of about 45GPa and 41GPa, respectively, by linear acoustics Table 11a).

	(GPa)	35d	90d	180d
(a)	CEMII-Si-ref	44.5 ±1.5	48.4 ±0.8	43.3 ±0.9
	CEMI-Ca-ref	40.9 ±0.6	41.6 ±0.5	41.9 ±0.2
(b)	CEMII-Si-ref	-	-	-
	CEMI-Ca-ref	33.5 ±0.5	34.6 ±0.4	35.1 ±0.7

Table 11: Evolution of the dynamic moduli in linear (a) and nonlinear (b) acoustics over time for reference concretes

The CEMII-Si and CEMII-Ca pathological concretes have dynamic moduli of 36 GPa and 39 GPa, respectively, and only the dynamic moduli of the CEMII-Si concrete seems to be impacted by the heat treatment. This difference can be explained by the difference of ITZ between these aggregates [21, 30]. For the pathological concretes, no evolution of the dynamic moduli measured by linear acoustics is observed during the expansion. When the damage becomes too great, during the acceleration phase, the received signal becomes too disturbed. It follows that a very weak signal is detected by the sensor in reception, making the measurements unusable (linear acoustics).

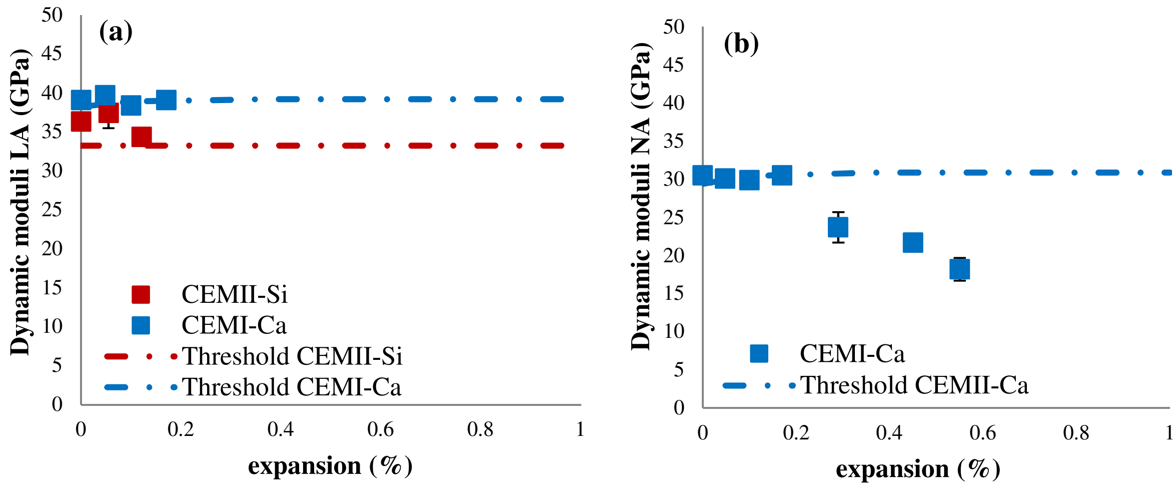

Figure 17: Evolution of the dynamic moduli in linear (a) and nonlinear (b) acoustics according to the expansion for concretes damaged by DEF

Dynamic moduli measurements in nonlinear acoustics (Figure 17b) show the same trend. The dynamic moduli remains stable around 35 GPa over time for the reference concrete (Table 11b). The dynamic moduli of the pathological concrete CEMI-Ca remains slightly lower than that of the reference concrete, 30 GPa at 35 days. However, it decreases rapidly around 0.2% of expansion during the acceleration phase of the pathology. The loss of moduli associated with the development of the DEF is of the order of 30% at 0.45% of expansion. These results are in agreement with those found in the literature [10, 31, 32, 33].

Depending on the criterion chosen, detection by nonlinear dynamic moduli takes place between 0.17 and 0.29% of expansion, at the beginning of the acceleration phase. The linear dynamic moduli does not allow DEF to be detected.

4. Discussion

4.1. Detection of DEF

The results obtained on the evolution of the concrete properties according to expansion show that only some particular tests make it possible to detect DEF at the beginning of the expansion, during the latent phase. Table 12 summarizes all the expansion values at the time of detection of pathologies presented in the experimental results.

	Expansion at detection (%)		DEF phase
	CEMII-Si	CEMI-Ca	
pH of pore solution	-	-	-
Portlandite content	-	-	-
Chloride migration	-	-	-
Electrical resistivity	0.05-0.11	0.05-0.11	Latent phase
Water porosity	0.11-0.25	0.17-0.29	Acceleration phase
Gas permeability	0.05	0.17-0.29	Latent phase
Dynamic moduli AL	-	-	-
Dynamic moduli NA	-	0.17-0.29	Acceleration phase
Static moduli	0.05 / 0.11	0.05-0.11	Latent phase
Compressive strength	0.11 / 0.25	0.17-0.29	Acceleration phase

Table 12: Summary of the evolution of the properties at detection for the CEMII-Si and CEMI-Ca concretes

Microscopic observations showed the evolution of ettringite formation during expansion in the material. However, measurements of pH and portlandite content showed no evolution during the expansion. The potential modification of portlandite when the pathology develops in the concrete cannot be identified by the technique used in this study. Some physical measurements related to the transfer properties allowed DEF to be detected during the latent phase and measurements of the gas permeability and electrical resistivity appear to provide a good sustainability indicator for the detection of DEF. The doubling of the apparent gas permeability coefficient at 0.12% of expansion for the CEMII-Si concrete reveals that the loss of containment occurs at a low degree of expansion for unreinforced concrete. However, the CEMI-Ca concrete showed a later increase in permeability coefficient, during the acceleration phase. The improvement of ITZ in the case of limestone aggregates seems to reduce the cracks generated at this interface during DEF damage [23]. Thus allowing the cracks in the concrete to be less percolating.

The electrical resistivity tests also showed significant sensitivity, the detection being effective from the latent phase. The electrical resistivity decreased by 16% and 10% for the CEMII-Si and CEMI-Ca concretes, respectively, for expansions of 0.12% and 0.19%. Since the electrical resistivity of the reference concretes increased substantially from 35 days to 180 days, the decrease in the resistivity associated with the development of the pathology seems to be significant. However, this parameter was very sensitive to the degree of saturation of concrete [34]. In case of existing structure, electrical resistivity is commonly used to assess the degree of saturation of concrete. So in case of DEF damage structure, it could be difficult to use the electrical resistivity to determine both the degree of saturation and the occurrence of DEF.

The water porosity measurements did not show any great sensitivity. The increase in porosity associated with micro-cracks in the matrix was small compared to the initial pore volume, making detection difficult. A relative increase of the porosity of 19% compared to the initial porosity for a swelling of 0.25% was observed on the CEMII-Si concrete. At this degree of expansion, cracking was already visible on the faces of the concrete specimens. Dynamic moduli measurements in linear acoustics did not detect the presence of DEF in concrete but tests in nonlinear acoustics showed a decrease in dynamic moduli when it was no longer measurable by the previous method. A decrease of 22% for an expansion of 0.29% was observed for the CEMI-Ca concrete at the middle phase of acceleration. Static moduli measurements had greater sensitivity than the two previous methods and allowed detection during the latent phase. A continuous decrease was observed throughout the development of the pathology. A 15% loss of moduli associated with a swelling of 0.11% was observed for each concrete. The compressive strength of the CEMII-Si and CEMI-Ca concretes damaged by DEF decreased by 26% and 14% respectively for expansions of 0.25% and 0.29%. This loss of compressive strength in the middle phase of acceleration delayed the detection of the pathology. Three sustainability indicators made it possible to detect DEF earlier, during the latent phase for laboratory specimens. These were the gas permeability, the electrical resistivity and the static moduli.

4.2. Sustainability of concretes damaged by DEF

Figure 18 shows the evolution of the damage as a function of the expansion for the two concretes undergoing DEF. In this study, the damage was proportional to the expansion due to DEF. The damage was calculated from the static moduli according to Equation 4:

$$D = 1 - \frac{E_i}{E_0} \quad (4)$$

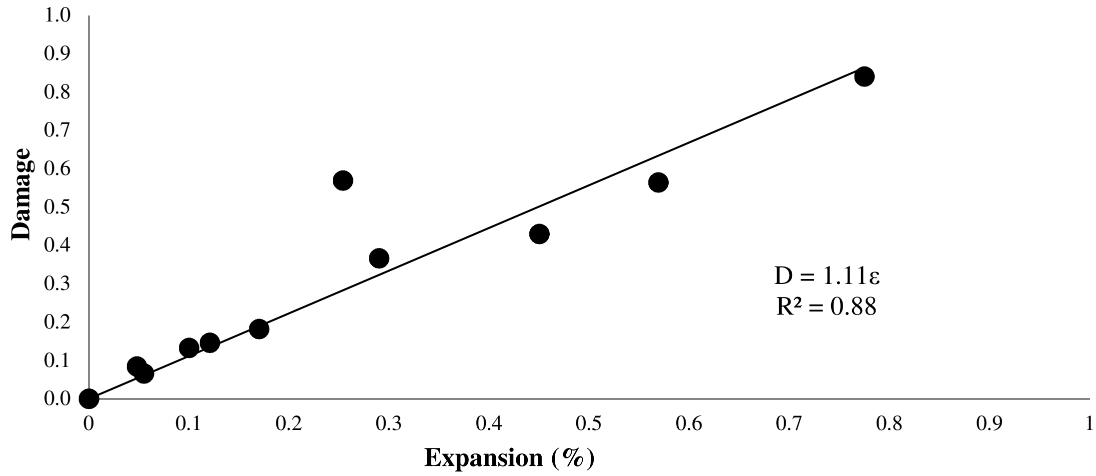

Figure 18: Evolution of the damage as a function of expansion

A study by Martin et al. on coupled AAR and DEF expansion on concrete shows an almost linear trend. The loss of damage according to the expansion is in accordance with these results [35].

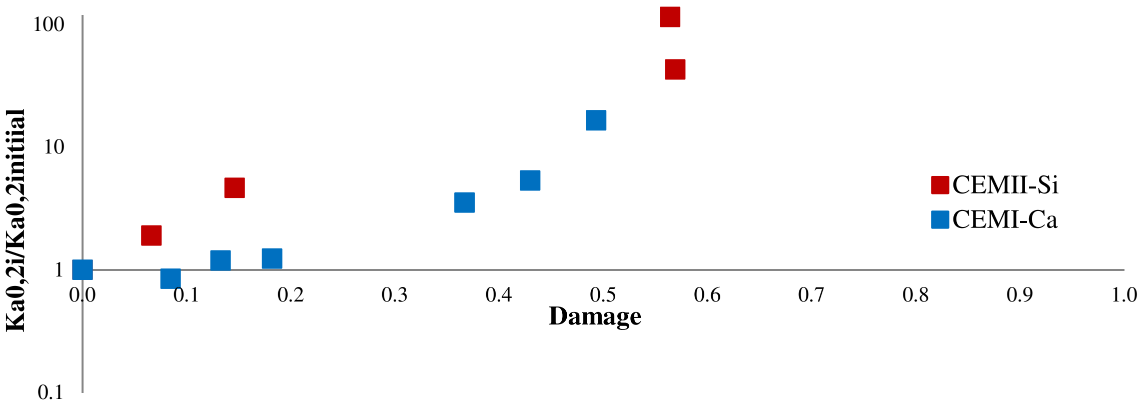

Figure 19: Evolution of the apparent permeability rate as a function of damage

The evolution of the apparent gas permeability rate presented in Figure 19 shows that the increase in the permeability seems to be an exponential function of the damage. However, the percolating paths in CEMI-Ca concrete specimens would appear at around 20% of damage, at the beginning of the acceleration phase of the pathology. For the CEMI-Si concrete, the percolating paths appear for slight damage, around 7%, causing a considerable increase of the air flow through the material. The greater bonding at the ITZ in the case of limestone aggregates seems to allow the containment properties to be maintained during the beginning of the DEF damage, when it is lower than 20%.

Potential Sustainability					
Sustainability indicators	**Concretes**	**Initial state**	**Latent phase**	**Acceleration phase**	**Stabilization phase**
Expansion (%)	**CEMII-Si**	**0**	**0.02-0.15**	**0.15-0.7**	**0.8**
	CEMI-Ca	**0**	**0.02-0.1**	**0.1-0.45**	**0.55**
Electrical resistivity	**CEMII-Si**	**Very low**	**Very low**	**Very low**	**Very low**
	CEMI-Ca	**Very low**	**Very low**	**Very low**	**Very low**
Gas permeability (40°C)	**CEMII-Si**	**Medium**	**Low**	**Very low**	**Very low**
	CEMI-Ca	**High**	**High**	**Medium**	**Low**
Water porosity (40°C)	**CEMII-Si**	**High**	**Medium**	**Low**	**Low**
	CEMI-Ca	**Medium**	**Medium**	**Low**	**Low**

Table 13: Classification of concrete damaged by DEF relative to limit values for the potential sustainability and properties of concrete [36]

Table 13 shows the evolution of the potential durability of concretes during the development of the pathology. The "low" classification at the initial state of concretes is mainly due to the effects of heat treatment and wet/dry cycles as mentioned previously [21, 29, 30]. Sustainability indicators show lower potential sustainability as early as the latent period for CEMII-Si concrete and this trend continues throughout the degradation. The presence of limestone aggregates in CEMI-Ca concrete seems to maintain the same sustainability during this phase. During the acceleration phase of the pathology, the potential sustainability of concretes becomes greatly affected. This could accelerate the kinetics of appearance of other pathologies such as AAR, carbonation and corrosion, causing premature aging of the structures.

5. Conclusion

A large experimental program has been proposed in order to obtain a sensitive measurement of DEF, allowing its detection before it can be observed visually. The second objective was to evaluate the evolution of the properties that have an impact on the containment and on the sustainability of concrete where other pathologies are also present. Numerous physicochemical and mechanical properties were measured by the use of a large quantity of samples. These tests were performed on two concretes showing a high swelling potential when DEF occurs and containing aggregates of different mineralogical natures. First, it confirms the results of the scarce studies reported in the literature:

- DEF expansion is isotropic in stress-free conditions [25].

- Microscopic observations have shown DEF development in accordance with the theory of swelling proposed by Brunetaud [1].

Second, original results have been obtained on the durability indicators for concrete damaged by DEF:

- The measurements of pH and portlandite content do not show any evolution during the pathology in spite of strong leaching of alkalis.
- The measurement of physical properties shows that electrical resistivity and gas permeability are sensitive to the expansion generated by DEF, the detection being effective from the latent period for laboratory specimens. However, the electrical resistivity could be difficult to use for damaged structures due to its sensitivity to other parameters [34]. Water-accessible porosity and chloride migration tests are not suitable for the detection of the pathology, their sensitivity being too low with respect to the presence of cracks through the cementitious matrix.
- For a given expansion, the permeability increase of concrete damaged by DEF is greater for concrete containing silica aggregate than for concrete with limestone aggregate.
- The mechanical tests show that, despite the filling of the ettringite cracking at the end of expansion, no improvement is observed in the measured properties. Only the measurement of the static moduli allows detection of the pathology during the latent period and shows that the loss of moduli seems to be proportional to the expansion measured in stress free conditions.
- Three sustainability indicators seem to allow the detection of pathology in the short term during the latent period: gas permeability, electrical resistivity, and static moduli.
- The loss of containment in case of nuclear power plants related to the presence of DEF depends of the nature of the aggregates and occurs for less than 20% of damage.
- At the acceleration phase, the potential sustainability of concretes is greatly altered and could lead to the premature appearance of other pathologies.
- The presence of limestone aggregates seems to improve the sustainability of concrete subject to DEF.

This study was performed on a large quantity of laboratory specimens in stress free swelling and fully saturated conditions. It is necessary to pursue the study to evaluate the influence of a larger volume of concrete, the presence of reinforcement and the presence of a water content gradient in order to detect DEF on existing structures. In the case of nuclear power plants, it is also necessary to develop nondestructive methods related to the properties sensitive to DEF proposed in this study in order to maintain the containment property of concrete. In this context, a test platform for the measurement of DEF sustainability indicators on concrete at structure scale is being developed in the ODOBA (Observatoire de la Durabilité des Ouvrages en Béton Armé) project.

Acknowledgment

The authors thank the Institute of Radioprotection and Nuclear Safety (IRSN) for its financial support.

References

[1] Brunetaud X., 2005. Etude de l'influence de différents paramètres et de leurs interactions sur la cinétique et l'amplitude de la réaction sulfatique interne au béton. PhD thesis, Ecole Centrale de Paris.

[2] Leklou N., Aubert J-E., Escadeillas G., 2013. Influence of various parameters on heat-induced internal sulphate attack. European journal of environmental and civil engineering. Vol. 17:3, p. 141-153. https://doi.org/10.1080/19648189.2012.755338.

[3] Zhang Z., Olek J., Diamond S., 2002. Studies on delayed ettringite formation in heat-cured mortars II. Characteristics of cement that may be susceptible to DEF. Cement and Concrete Research. Vol. 17, p. 1737-1742. https://doi.org/10.1016/S0008-8846(02)00894-3.

[4] Petrov N., 2003. Effets combinés de différents facteurs sur l'expansion des bétons causés par la formation différée de l'ettringite. PhD thesis, Université de Sherbrooke.

[5] Grattan-Bellew P.E., Beaudoin J.J., Vallée V.G., 1998. Effect of aggregate particle size and composition on expansion of mortar bars due to delayed ettringite formation. Cement and Concrete Research. vol. 28, n° 8, p. 1147-1156. https://doi.org/10.1016/S0008-8846(98)00084-2.

[6] Fu Y., Ding J., Beaudoin J. J., 1997. Expansion of Portland cement mortar due to internal sulfate attack. Cement and Concrete Research. Vol. 27, p. 1299-1306. https://doi.org/10.1016/S0008-8846(97)00133-6.

[7] Graf L., 2007. Effect of Relative Humidity on Expansion and Microstructure of Heat-Cured Mortars. RD139. Portland Cement Association. Skokie, Illinois. 50 pages.

[8] Al Shamaa M., 2012. Etude du risque de développement d'une réaction sulfatique interne et de ses conséquences dans les bétons de structure des ouvrages nucléaires. PhD thesis, Université Paris-Est.

[9] Kchakech B., 2016. Etude de l'influence de l'échauffement subi par un béton sur le risque d'expansions associées à la réaction sulfatique interne. PhD thesis, Université Paris-Est.

[10] Al Shamaa M., Lavaud S., Divet L., Nahas G., Torrenti J.-M., 2014. Coupling between mechanical and transfer properties and expansion due to DEF in a concrete of a nuclear power plant. Nuclear Engineering and Design. Vol. 266, p. 70-77. https://doi.org/10.1016/j.nucengdes.2013.10.014.

[11] Jabbour J., 2018. Méthodes d'essais de vieillissement accéléré des bétons à l'échelle des ouvrages. PhD thesis, Université Paris-Saclay.

[12] NF P18-400, 1981. Bétons - Moules pour éprouvettes cylindriques et prismatiques.

[13] NF P18-404,1981. Bétons - Essais d'étude, de convenance et de contrôle - Confection et conservation des éprouvettes.

[14] Méthode d'essai n°66, 2007. Réactivité d'un béton vis-à-vis d'une reaction sulfatique interne. Laboratoire Central des Ponts et Chaussées.

[15] PerfDuB, 2017. Determination of the resistivity of saturated concrete.

[16] XP P 18-461, Testing hardened concrete — Non-steady state chloride migration test – Determination of effective chloride migration coefficient

[17] XP P18-463, 2011. Bétons - Essai de perméabilité aux gaz sur béton durci.

[18] NF P18-549, 2010. Béton - Essai pour béton durci - Essai de porosité et de masse volumique.

[19] NF EN 12390-3, 2003. Essais pour béton durci - Partie 3: résistance à la compression des éprouvettes.

[20] NF EN 12390-13, 2014. Essai pour béton durci - Partie 13: détermination du module sécant d'élasticité en compression.

[21] Al Shamaa M., Lavaud S., Divet L., Colliat J .-B., Nahas G., Torrenti J.-M., 2016. Influence of limestone filler and of the size of the aggregates on DEF. Cement and Concrete Composites. Vol 71, p. 175-180. https://doi.org/10.1016/j.cemconcomp.2016.05.007

[22] Bentz D., Ardani A., Barrett T., Jones S., Lootens D., Peltz M., Sato T., Stutzman P., Tanesi J. and Weiss J., 2015. Multi-scale investigation of the performance of limestone in concrete. Construction and Building Materials. Vol. 75, p. 1-10. http://dx.doi.org/10.1016/j.conbuildmat.2014.10.042.

[23] Yang R., Lawrence C. D., Sharp J.H., 1999. Effect of type of aggregate on delayed ettringite formation. Advances in Cement Research. Vol. 11, n°3, p. 119-132. https://doi.org/10.1680/adcr.1999.11.3.119.

[24] Tosun K. and Baradan B., 2010. Effect of ettringite morphology on DEF-related expansion. Cement and Concrete Composites. Vol. 32, p. 271-280. https://doi.org/10.1016/j.cemconcomp.2010.01.002.

[25] Bouzabata H., Multon S., Sellier A., Houari H., 2012. Effects of restraint on expansion due to delayed ettringite formation. Cement and Concrete Research. Vol. 42, p. 1024–1031. https://doi.org/10.1016/j.cemconres.2012.04.001.

[26] Sagüés A.A., Moreno E.I., and Andrade C., 1997. Evolution of pH during in-situ leaching in small concrete cavities. Cement and Concrete Research. Vol. 27, n° 11, p. 1747-1759. https://doi.org/10.1016/S0008-8846(97)00177-4.

[27] Chappex T., and Scrivener K., 2012. Alkali fixation of C–S–H in blended cement pastes and its relation to alkali silica reaction. Cement and Concrete Research. Vol. 42, p.1049-1054. https://doi.org/10.1016/j.cemconres.2012.03.010.

[28] Thibaut Y., 2018. Evaluation des structures en béton armé atteintes de réaction sulfatique interne. PhD thesis, Université Toulouse 3.

[29] Gallucci. E.. Zhang. X. and Scrivener. K. L., (2013). Effect of temperature on the microstructure of calcium silicate hydrate (C-S-H). Cement and Concrete Research. Vol. 53, p. 185-195. https://doi.org/10.1016/j.cemconres.2013.06.008.

[30] Cagnon. H., Vidal. T., Sellier. A., Bourbon. X. and Camps, G., 2015. Drying creep in cyclic humidity conditions. Cement and Concrete Research. vol. 76, p. 91-97. https://doi.org/10.1016/j.cemconres.2015.05.015.

[31] Al Shamaa M., Lavaud S., Divet L., Nahas G., Torrenti J.-M., 2015. Influence of relative humidity on delayed ettringite formation. Cement and Concrete Composites. Vol. 58, p. 14-22. https://doi.org/10.1016/j.cemconcomp.2014.12.013.

[32] Brunetaud X., Divet L., Damidot D., 2008. Impact of unrestrained Delayed Ettringite Formation-induced expansion on concrete mechanical properties. Cement and Concrete Research. Vol. 38, p. 1343–1348. https://doi.org/10.1016/j.cemconres.2008.05.005.

[33] Pavoine A., Brunetaud X., Divet L., 2012. The impact of cement parameters on Delayed Ettringite Formation. Cement and Concrete Composites. Vol. 34, p. 521-528. https://doi.org/10.1016/j.cemconcomp.2011.11.012

[34] Rivard P., Saint-Pierre F., 2009. Assessing alkali-silica reaction damage to concrete with non-destructive methods: From the lab to the field. Construction and Building Materials. Vol. 23, p. 902–909. https://doi.org/10.1016/j.conbuildmat.2008.04.013.

[35] Martin R.-P., Sanchez L., Fournier B., Toutlemonde F., 2017. Evaluation of different techniques for the diagnosis & prognosis of Internal Swelling Reaction (ISR) mechanisms in concrete. Construction and Building Materials. Vol. 156, p. 956–964. https://doi.org/10.1016/j.conbuildmat.2017.09.047.

[36] Baroghel-Bouny V. et al., 2004. Conception des bétons pour une durée de vie donnée des ouvrages. Maîtrise de la durabilité vis-à-vis de la corrosion des armatures et de l’alcali-réaction. Etat de l’art et guide pour la mise en œuvre d’une approche performantielle et prédictive sur la base d’indicateurs de durabilité. Guide AFGC.